Standard Issue – Article

Journal of Agricultural Engineering

https://www.agroengineering.org/

Development of high-speed and precision metering device with gradient-feeding and control seed for soybean planting

Xuhui Chen, Shilin Zhang, Jianxin Dong, Fang Liu, Xian Jia, Yuxiang Huang

Please cite this article as doi: 10.4081/jae.2024.1574

Submitted: 01/11/2022
Accepted: 27/04/2023

Development of high-speed and precision metering device with gradient-feeding and control seed for soybean planting

Xuhui Chen, Shilin Zhang, Jianxin Dong, Fang Liu, Xian Jia, Yuxiang Huang

School of Mechanical and Electronic Engineering, Northwest Agriculture and Forestry University, Yangling, China

Correspondence: Huang, Yuxiang, Northwest A&F University College of Mechanical and Electronic Engineering, Yangling, China Yanling 712100, China.
E-mail: hyx@nwsuaf.edu.cn

Key words: bench test; control-seed; gradient-feeding; high-speed and precision; seed metering devices; simulation.

Acknowledgments: this work was supported by the National Natural Science Foundation of China (Grant No. 31971802) and National Key R&D Program of China (2021YFD2000405).

Conflict of interest: the authors declare no potential conflict of interest.

Abstract

High-speed and precision planting was employed to improve the yields of soybean seeds. However, most mechanical seed metering devices had a lower quality index under high-speed. In this study, a high-speed and precision metering device with gradient-feeding (GF) and control-seed (CS) for soybean planting was designed to improve the quality index at high speeds. GF was designed to make soybean seeds rapidly enter seed cells. CS prevented soybean seed that was to be released from being cleared during the clearing stage. Firstly, the range of working parameters of it was determined by theoretical analysis, which included the angle of guiding-slope (α), the angle of seed-control (θ), and mutation height (ΔH). Then, orthogonal center combination tests with three-factor and five-level were carried out to determine the corresponding quality index and miss index with different working parameters. The optimal working parameters were determined by regression equations between the quality index and the miss index. The high-speed and precision metering device with GF and CS was thus manufactured based on these optimal working parameters. The simulation test and bench test of it were carried out with different forward speeds of the planter. The results showed that the optimal angle of guiding-slope (α), angle of seed-control (θ), and mutation height (ΔH) were 18.06°, 136.67°, and 2.77 mm, respectively. In the bench test, all quality indices were higher than 95.00%, and all miss indices were lower than 3.00% when the forward speed of the planter was 4 - 16 km/h. The results of the bench test were consistent with the results of the simulation test, with an average relative error of 2.33%. High-speed and precision metering device with gradient-feeding (GF) and control-seed (CS) can realize precision planting at high speeds.

Introduction

High-speed and precision planting was the development direction and trend of modern planting technology. High-speed planting sowed more seeds in the same amount of time as low-speed planting with less costs (Kostic et al., 2018). Precision planting was able to sow more densely, which thus reduced plant spacing (Ahmadi et al., 2008; Wang et al., 2022). High-speed and precision planting realized large-scale production and improved yields (Wang et al., 2022; Wang et al., 2021; Koller et al., 2014).

High-speed and precision metering device was critical equipment for high-speed and precision planting (Zhao et al., 2022). Most mechanical seed metering devices were designed for low-speed

conditions, which were lower than 8 km/h (Xue et al., 2019; Chen et al., 2017). However, most of them had a lower quality index with high-speed, which was more than 8 km/h. Consequently, the high-speed and precision metering device was urgently designed to enhance yields and reduce planting costs.

The working stage of the high-speed and precision metering devices was divided into feeding, clearing, protecting, and releasing stages (Jia et al., 2018). The feeding stage was an initial working stage, which made seeds enter seed cells (Cay et al., 2018). The clearing stage ensured that the only seed to be released was not cleared in this stage (Ryu and Kim, 1998). It was essential in determining whether the seed metering devices successfully rowed. The feeding and clearing stages greatly impacted the working performance of the high-speed and precision metering device.

Relevant scholars had a lot of research on improving the working performance of the feeding stage. The seed population density changed the working performance of feeding seeds (Correia et al., 2016; Du et al., 2019; Xing et al., 2020; Zhao et al., 2020). Xue et al. (2019) designed a double-curved guiding groove to make seeds enter the seed cell orderly. Li et al. (2020) used the "Y" type of seed guiding groove structure to increase the fluidity of seeds. Above studies mainly focused on changing seed population density or orderly arranging seeds to improve the performance of feeding seeds. However, their studies could not reduce the time for seeds to enter the seed cell, which thus was not employed under high-speed conditions. Therefore, gradient-feeding (GF) structure was designed to feed seeds rapidly.

Some researchers studied how to improve the working performance of the clearing stage. Wang et al. (2017) improved the effect of seed clearing by changing the stress force of seeds. Hu et al. (2022) designed a double-sided seed-cleaning mechanism to improve the performance of clearing seeds. Yazgi and Degirmencioglu (2007) optimized the vacuum of the seed metering device to improve the performance of clearing seeds. Xiong et al. (2021) adopted an air-blowing type to clear seeds. However, in the above study, the seed to be released might fall in the clearing stage. Therefore, this study designed a control-seed (CS) structure to reduce the phenomenon of over-clearing during the clearing stage.

The objectives of this study were to (1) design a high-speed and precision metering device with GF and CS, (2) determine the range of working parameters of GF and CS structure by theoretical analysis, (3) determine the optimal working parameters through simulation, and (4) validate

simulation results by bench tests.

Materials and Methods

Structure of high-speed and precision metering device

The soybean seed precision metering device with GF and CS was designed for high-speed conditions. It was mainly composed of a seed feeding tube, front shell, seed-taking wheel, fixed limiting ring, adjusting limiting ring, transmission shaft, and rear shell (Figure 1a). A double chamber structure of the seed cell was adopted in the seed cell of the high-speed and precision metering device with GF and CS, which included a seed-feeding chamber and a seed-releasing chamber (Figure 1b). GF was realized by the guiding-slope and arc surface role in the seed-feeding chamber, which made soybean seeds quickly enter the seed-releasing chamber.

The seed-taking wheel was located in the middle of the transmission shaft, driven by the transmission shaft. Seed cells were distributed evenly inside the seed-taking wheel. The fixed limiting ring and adjusting limiting ring were arranged outside the seed-taking wheel, connected by bolts. CS restricted soybean seeds in a confined space under the mutated structure of adjusting limiting ring and the seed-releasing chamber of the seed-taking wheel (Figure 1c). They limited the internal position of the seed cells and thus restricted soybean seeds.

Working principle of high-speed and precision metering device

The working process of the high-speed and precision metering device with GF and CS was divided into four stages: feeding stage, clearing stage, protecting stage, and releasing stage, as shown in Figure 2. Firstly, soybean seeds entered the high-speed and precision metering device from the seed feeding tube. Then, the soybean seed population formed inside the high-speed and precision metering device. It was divided into soybean seeds to be released and soybean seeds to be cleared. When the high-speed and precision metering device started to work, the seed-taking wheel turned clockwise. Soybean seeds to be released would complete four stages with rotation of the seed-taking wheel.

During the feeding stage, soybean seeds were arranged in a row at the front of the seed-feeding chamber of seed cells. Soybean seeds that were first fed in seed cells were soybean seeds to be released. Others were soybean seeds to be cleared. Soybean seeds to be released entering the seed-feeding chamber were quickly guided into the seed-releasing chamber under the guidance of the

guiding-slope. Soybean seeds to be released at this point completed the feeding stage.

Soybean seeds to be cleared started to fall due to gravity during the cleaning stage. Soybean seeds to be released were restrained in the seed-releasing chamber under the mutation structure. Soybean seeds to be cleared in the seed-feeding chamber were cleared from seed cells by gravity. Soybean seeds to be released completed the clearing stage.

In the protection stage, soybean seeds to be released in the seed-releasing chamber fell from the rear end of the seed-releasing chamber to the front end of the seed-releasing chamber under the action of gravity. This process made soybean seeds to be released reduce the impact on the rear end of the seed-releasing chamber and thus the fluctuation of releasing trajectory. Soybean seeds to be released were stabilized at the front of the seed-releasing chamber, which thus completed the protection stage.

In the releasing stage, there was not an adjustment limiting ring at the bottom of the seed-releasing chamber. Soybean seeds to be released in the seed-releasing chamber left the seed cells under the force of gravity and then fell to the ground. Soybean seeds to be released at this point completed the releasing stage.

Determination of structure parameter

Structure of seed cell

The seed cell was the key structure of the seed-taking wheel, whose size was determined by Equation (1). A 45 ° inclined side plate was designed at the opening of the seed-feeding chamber to destroy the force chain network of soybean population (Xue et al. 2019). The width and height of the opening of seed-feeding were determined to ensure that only one row of soybean seeds entered the seed-feeding chamber each time. The range of width L_1 of the opening of seed-feeding was $1.2d_{max}$ - $2d_{min}$. The range of height L_2 of the opening of seed-feeding was $1.2d_{max}$ - $2d_{min}$. The angle of top slope α was equal to the angle of bottom slope to ensure that only one soybean seed passed through the internal space of seed-feeding chamber. The height L_3 between the two slopes was consistent with the height L_2 of the opening of seed-feeding chamber.

An arc surface was designed at the rear end of the seed-feeding chamber. It made soybean seeds smoothly enter the seed-releasing chamber during the feeding stage. Its radius R was more than $2d_{min}$, which was determined by preventing more than one soybean seed from simultaneously passing through the seed-feeding chamber. The length L_4 of the seed-releasing chamber was more

than $1.5\mathrm{d}_{max}$ to minimize collision between soybean seeds and the inner wall of the seed-releasing chamber.

$$\begin{cases} 1.2\mathrm{d}_{max} \le \mathrm{L}_1 \le 2\mathrm{d}_{min} \\ 1.2\mathrm{d}_{max} \le \mathrm{L}_2 \le 2\mathrm{d}_{min} \\ \mathrm{L}_3 = \mathrm{L}_2 \\ \mathrm{L}_4 \ge 1.5\mathrm{d}_{max} \\ 1.2\mathrm{d}_{max} \le R \le 2\mathrm{d}_{min} \end{cases} \quad (1)$$

Where d_{max} and d_{min} are the maximum and minimum equivalent diameter of soybean seeds, respectively (mm) (Table 2).

Distribution of seed cell

The seed cell was the main structure of the seed-taking wheel. According to Agricultural Machinery Design Manual (China Agricultural Science and Technology Press Pub. Date: 2007-10-1, 2000), the diameter of the seed-taking wheel D was 245 mm. The bottom thickness of the seed cell was 10 mm to realize CS function. Therefore, the circle distributed diameter D_0 of the seed cell was 225 mm by calculating the difference of diameter of the seed-taking wheel and twice the bottom thickness of the seed cell.

The number of seed cells distributed on the seed-taking wheel affected the efficiency of feeding soybean seeds. The forward speed of the planter was calculated by Equation (2). To maintain the same plant spacing with a certain speed of planter, the number of the seed cell was inversely proportional to the speed of the transmission shaft. Therefore, arranging as many seed cells as possible was necessary to meter more soybean seeds.

$$v = \frac{6zhn}{10000} \quad (2)$$

Where v is the forward speed of the planter (km/h), h (10 cm) is planting distance, n is the speed of the seed-taking wheel (r/min), z is the number of seed cells.

The number of seed cells was determined by simplifying the feeding stage, as shown in Figure 4. When more than half of the equivalent diameter of one soybean seed was in the range of the seed-feeding chamber opening, it was successfully fed (Chen et al., 2017). The distance between seed cells was determined by Equation (3).

According to Equations (2) and (3), the number of seed cells was 20, which was calculated by Equation (4). At the same time, a double-circle seed-taking wheel was designed by staggering two single-circle seed-taking wheels to realize higher speed. The seed-taking wheel adopted an

axisymmetric staggered arrangement of seed cells to increase the number of seed cells (Figure 1b). Therefore, the number of seed cells in the seed-taking wheel was 40, twice that of the single-circle seed-taking wheel.

$$\begin{cases} t = \sqrt{\frac{d_{max}}{g}} \\ L = v_0 t \\ l \geq L + 0.5d_{max} + L_c \\ v_0 = \omega \frac{D_0}{2} = \frac{\pi n D_0}{60} \\ l \approx \frac{\pi D_0}{z} \\ l \geq L_4 \end{cases} \quad (3)$$

$$z \leq \frac{60\pi}{\pi n \sqrt{\frac{d_{max}}{g}} + \frac{90 d_{max}}{D_0}} \quad (4)$$

Where t is the time of one soybean seed dropped $0.5d_{max}$ in the vertical direction, and L is the corresponding horizontal movement distance of this soybean seed within t, and g is gravitational acceleration, l is the distance between the seed cells (mm), and v_0 is the linear speed of the seed cell (m/s), and L_c is the length of the seed-taking chamber, and ω is the angular velocity of the seed cell (rad/s), and D_0 is diameter of the circle where the seed cell is located (mm).

Structure of control-seed

The vibration load on the seed cell increased with high-speed (Du et al., 2013). CS was designed to constrain soybean seeds in the clearing stage under the vibration load. The angle of control-seed θ was angle from OO_1 to starting position of the mutation structure, as shown in Figure 5a. OO_1 was a line segment in the vertical direction. The mutation structure of adjusting limiting ring was employed to constrain soybean seeds in the seed-releasing chamber, which prevented them from falling out of the seed-releasing chamber in the cleaning stage.

CS included seed cell, fixed limiting ring, and adjusting limiting ring (Figure 5b). The structure of CS was determined by Equation (5). Both the height L_6 of the seed-releasing chamber and the width L_5 of the fixed limiting ring were more than d_{max} to ensure that soybean seed was able to enter the seed-releasing chamber, as shown in Figure 5c. Protrusion thickness H of the fixed limiting ring increased with angle of the guiding-slope α. It decreased with the angle of the guiding-slope α. ΔH was the difference between the protrusion thickness H of the fixed limiting ring and the protrusion thickness H_t of the adjusting limiting ring. ΔH was less than d_{min}, which prevented soybean seed

from leaking out of or seizing in the gap between the seed cells and the fixed limiting ring.

$$\begin{cases} L_5 \geq d_{max} \\ L_6 \geq d_{max} \\ H_t = H + \Delta H \\ \Delta H \leq d_{min} \\ \Delta H = L_1 \tan \alpha \end{cases} \quad (5)$$

Determination of working paraments

Analysis of GF process

The GF process was the process of achieving rapid seed feeding at high speeds. Based on the structure of the double chamber, the GF process in the feeding stage was for force analysis. Firstly, one seed cell was taken for analysis, whose position was in the range of the angle of control-seed, as shown in Figure 6a. The angle between this seed cell and the starting position of the angle of control-seed was φ. Three-dimensional coordinate system was established on this seed cell, as shown in Figure 6b. The x-axis direction was the same as the linear speed direction of the seed-taking wheel. The y-axis direction was always from this seed cell to the front shell of high-speed and precision metering device. The z-axis direction was always from this seed cell to the center of seed-taking wheel.

In the three-dimensional coordinate system of the seed cell, the soybean seed to be released was mainly affected by the force of the soybean seed to be cleared, the support force of the seed cell, the friction force of the seed cell, gravity and centrifugal force (Figure. 6b). The position status of the seeds to be released and cleared was shown by three two-dimensional diagrams, as shown in Figure 6(c - e). According to the position relationship of the seed cell, the dynamic Equation (6) of the soybean seed to be released can be obtained.

$$\begin{cases} 0 \leq \varphi \leq \theta \\ ma = F_1 + F_2 + F_3 + f_2 + f_3 + F_n + G \\ f_2 = \mu F_2 \\ f_3 = \mu F_3 \end{cases} \quad (6)$$

Where m is the mass of the soybean seed to be released (kg). a is the acceleration vector of soybean seed to be released in the three-dimensional coordinate system. F_1 is the force of the soybean seed to be cleared to the soybean seed to be released (N). F_2 is the supporting force of the side arc surface of the seed cell to the soybean seed to be released (N). F_3 is the supporting force of the guiding-slope of the seed cell to the soybean seed to be released (N). f_2 is the friction force of the soybean seed to be released by the side arc surface of the seed cell (N). f_3 is the friction force of

the soybean seed to be released by the guiding-slope (N). F_n is the centrifugal force of the soybean seed to be released (N). G is the gravity component of the soybean seed to be released (N). μ is the friction coefficient between soybean seed and seed cell.

In Equations (6), the magnitude and direction of F_1 and the direction of F_{n} were related to φ. The magnitude and direction of F_2 and F_3 were related to θ. The magnitude and direction of f_2 and f_3 were related to F_2 and F_3, respectively. Therefore, the structure of the GF process was able to be determined by α and θ.

Analysis of CS process

CS process was to restrict the space of soybean seed to be released in the seed-releasing chamber. Each soybean seed to be released was kept in the seed cell, which had stable seed protection during the clearing stage. The force analysis of CS process was carried out by combining with its structure. Under the action of the seed-releasing chamber and the adjusting limiting ring, the stress state of soybean seeds to be released in the seed-releasing chamber met Equation (7). It formed a movement trend of pushing soybean seeds to be released to the top of the seed-releasing chamber, as shown in Figure 7. CS was achieved by constraining soybean seeds to be released in the confined space, formed by the seed-releasing chamber and the adjusting limiting ring. γ was the angle between F_4 and horizontal direction, which was related to θ (Figure 7). δ was angle between F_5 and horizontal direction, which was related to ΔH. All physical quantities involved in Equations (7) and (8) were related to θ and ΔH. Consequently, θ and ΔH were key parameters in the CS process.

$$\begin{cases} ma_k \cos\beta = F_4 \cos\gamma + F_5 \cos\delta - F_n \cos(90° - \gamma) - f_3 \cos(90° - \gamma) - f_4 \cos(90° - \delta) \\ ma_k \sin\beta = G + F_5 \sin\delta - F_4 \sin\gamma - F_n \sin(90° - \gamma) - f_3 \sin(90° - \gamma) + f_4 \sin(90° - \delta) \end{cases} \quad (7)$$

$$\begin{cases} f_4 = \mu F_4 \\ f_5 = \mu F_5 \\ G = mg \\ \gamma = 180° - \varphi \end{cases} \quad (8)$$

Where a_k is the acceleration of the soybean seed to be released (m/s^2). β is the angle between a_k and horizontal direction (°). F_4 is the support of the seed-releasing chamber to the soybean seed to be released (N). γ is F_4 included angle with horizontal direction (°). F_5 is the force of adjusting limiting ring to the soybean seed to be released (N). δ is F_5 included angle with horizontal direction (°). f_4 is the friction force of the soybean seed to be released by the seed-releasing chamber (N). f_5 is the friction force of the adjusting limiting ring for the soybean seed to be released (N). G is the

gravity of the soybean seed to be released (N).

Simulations

Model inputs

Engineering discrete element method (EDEM, ver. 2.7, https://www.edemsimulation.com) was used to conduct a virtual simulation of the working process of high-speed and precision metering device with GF and CS (Gao et al., 2020). The physical parameters of materials and seed metering devices need to be determined to input the EDEM software. Some variable physical parameters referred to previous studies, as shown in Table 1 (Liu et al., 2015; Shen et al., 2021). Digital modeling of the high-speed and precision metering device with GF and CS was carried out in the Inventor software, whose format file was imported into the EDEM software (Figure 8).

Physical parameters of soybean seeds were also determined to establish a simulation model of soybean seeds in the EDEM software. Therefore, the physical parameters of one thousand soybean seeds were randomly selected to measure and record. The variety of soybean seeds was "Suinong 26". The physical parameters involved length, width, height, and weight (Khatchatourian et al., 2014). Each measurement was repeated three times. The average value was calculated as the Ground Truth. The physical parameters of soybean seeds were shown in Table 2, of which the average weight was 232.2 g.

According to the physical parameters of soybean seeds, four basic ball units with a radius of 3.312 mm were cross-spliced into an assembly in the EDEM software, as shown in Figure 8 (Liu et al., 2015). Hertz-Mindlin (no-slip) model was used to input the EDEM software as a seed-seed contact model (Xue et al., 2020). Consequently, the digital modeling of soybean seed was determined in the EDEM software (Sharaby et al., 2022).

Simulations output

Different structure parameters affected the planting performance of high-speed and precision metering device with GF and CS (He et al., 2022; Hu et al., 2021). The critical structure parameters of the high-speed and precision metering device were determined by GF and CS structures, which included the angle of guiding-slope α, the angle of control-seed θ, and the mutation height ΔH, respectively. The range of the angle of guiding-slope was 0° - 25°. The range of the angle of control-

seed was 90° - 180°. The range of mutation height ΔH was 2 mm - 5 mm.

Orthogonal center combination tests with three-factor and five-level critical working parameters were conducted. When inputting the range of α, θ, and ΔH into the Design-Expert 8.0.6, their ranges were divided into five levels (Table 3). Twenty groups of different structure parameter combinations were determined by Central Composite Design. Then, the quality index and the miss index were determined by simulation in the EDEM software with different structure parameter combinations. The forward speed of the planter was set as 8 km/h. The corresponding speed of the seed-taking wheel was 33.33 rpm (Equation 2). For each structure parameters combination, three hundred soybean seeds were metered in the EDEM software (Shen et al., 2021). Each simulation was repeated three times and averages of the quality index and the miss index were regarded as the Ground Truth.

Response surface was determined by analyzing the result of 20 groups of different structure parameter combinations. The optimal values of structure parameters were thus determined when the quality index was the maximum value and the miss index was the minimal value on the response surface. After the optimal values of structure parameters were set, corresponding quality indices and miss indices when the forward speed of the planter was integer from 4 km/h to 16 km/h were able to determine in the EDEM software.

Performance of simulations

The Chinese Testing Standard for Precision Seeding recommended the quality index and the miss index as indicators for evaluating the performance of high-speed and precision metering device with GF and CS (GB/T6973-2005). In this study, the quality index I_q (%) and the miss index I_m (%) were calculated by Equation (9).

$$\begin{cases} I_q = \frac{M_1}{M} \times 100\% \\ I_m = \frac{M_2}{M} \times 100\% \end{cases} \quad (9)$$

Where M is the total number of metering seeds, M_1 is the qualified number of metering seeds, and M_2 is the missed number of metering seeds.

Bench tests

A bench test was carried out on the performance test system of a seed metering device (JPS-12) in

the Agricultural Machinery Laboratory of Northwest A & F University. A model of the designed high-speed and precision metering device was 3D printed, determined by the optimal parameter combination obtained by simulation in the EDEM software (Figure 9a). The model of the high-speed and precision metering device was placed on the JPS-12. The transmission shaft turned clockwise with a motor that was controlled by the controller. The speed of the transmission shaft was thus adjusted by the controller. Another side of the transmission shaft was connected with the seed-taking wheel. The speed of the oil belt on the JPS-12 was the same as the motor speed. After the oil belt started moving, the oil pump opened and then the controller worked. When the oil belt was covered with soybean seeds, the controller, oil pump, and oil belt were sequentially turned off.

When the forward speed of the planter was integer in 4 km/h - 16 km/h, the quality index and miss index of the high-speed and precision metering device were tested. Different speeds of the planter were repeated three times. Then, the distance between the soybean seeds to be released was measured with a ruler (Figure 9c). According to Chinese National Standard JB/T10293-2011 (Specifications for single-seed drills), the qualified distance of metering seeds was 0.5 - 1.5 times the standard distance (10 cm, Equation 2). This soybean seed was missed if the distance of metering seeds was more than 1.5 times the standard distance. Since the maximum measurement speed of JPS-12 was 12 km/h, when the forward speed of the planter was 13 km/h - 16 km/h, the speed of the oil belt was adjusted to 6.5 km/h - 8 km/h. The standard soybean spacing was 5cm to measure accordingly. Consequently, corresponding quality indices and miss indices were thus determined under different forward speed of the planter.

Results and Discussion

Simulation results

Simulation results obtained from the orthogonal center combination tests with three-factor and five-level were shown in Table 4. Combination 10 got the highest I_q (98.67%), while combination 14 got the lowest I_q (53.33%). Therefore, the angle of control-seed θ had little effect on I_q because both angles of control-seed θ of combinations 10 and 14 were 135°. Combination 5 got the highest I_m (27.67%), while combination 10 got the lowest I_m (0.67%). In combinations 5 and 10, three working parameters were not the same, indicating that all of them had a greater impact on I_m. Simulation results of Table 4 were input to Design-Expert 8.0.6 software to obtain the regression

models of quality index and miss index, which were shown in Equations (10) and (11), respectively.

$$I_m = 3.64 - 5.22A - 1.58B + 5.86\mathrm{C} + 0.75\mathrm{AB} - 4.50\mathrm{AC} - 0.67\mathrm{BC} + 2.01\mathrm{A}^2 + 0.59B^2 + 2.42C^2 \quad (10)$$

$$I_q = 96.37 + 5.35\mathrm{A} + 1.90\mathrm{B} - 10.91\mathrm{C} - 1.25\mathrm{AB} + 4.25\mathrm{AC} - 2.50\mathrm{A}^2 - 0.91\mathrm{B}^2 - 8.57\mathrm{C}^2 \quad (11)$$

Optimal values of design parameters

Variance analysis and significance test of the regression coefficient of the above regression models were carried out in the Design-Expert 8.0.6 software (Table 5). Both "Prob > F" values of I_q and I_m (< 0.0001) indicated that both of their models were significant. Both "Lack of Fit" values of I_q (0.0651 > 0.05) and I_m (0.5216 >0.05) implied their "Lack of Fit" were not significant. Both of "Prob > F" values of I_q and I_m were less than 0.0001 only under the interaction between α and ΔH. Therefore, the response surface was determined by the interaction between α and ΔH.

The response surface of the interaction between α and ΔH was obtained through the Design-Expert 8.0.6 software to analyze the further impact of working parameters on the quality index and miss index (Figure 10). The optimal value of α, θ, and ΔH were 18.06°, 136.67°, and 2.77mm, respectively. When working parameters were optimal under the forward speed of the planter was set as 8 km/h, the corresponding quality index and miss index of the simulation were 99.56% and 0.41%, respectively. The quality index first increased and then decreased as α and ΔH increased, while the miss index first decreased and then increased.

When α was fixed, the quality index first increased and then decreased with ΔH increased. The space of the seed-releasing chamber increased with ΔH increased. The soybean seed to be released was hardly to fall out from the seed-releasing chamber in the clearing stage. Therefore, the quality index was higher while the miss index was lower. However, the gap between the seed cell and the fixed limiting ring also got bigger and soybean seeds thus might be stuck in this gap when ΔH continued to increase. Therefore, the quality index decreased while the miss index increased when ΔH continued to increase.

When ΔH was fixed, soybean seeds were able to be more quickly fed with the action of the guiding-slope with α increased. However, the internal space of the seed cell became larger with α increased. More than one soybean seeds might be fed in seed-feeding chamber simultaneously. They might be stuck in the seed-feeding chamber and thus could not enter the seed-releasing chamber.

More than one soybean seeds also might simultaneously enter the seed-releasing chamber. Therefore, the quality index decreased while the miss index increased when α increased.

Results of bench test

The results of the bench test were shown in Figure 11. It showed that the quality index and the miss index of high-speed and precision seed metering device were 98.67% and 1.00% when the forward speed of the planter was 8 km/h, respectively. The quality indices were slightly lower than the corresponding simulation value when the forward speed of the planter was from 4 km/h to 16 km/h. The miss indices were higher than corresponding simulation value when the forward speed of the planter was from 4 km/h to 16 km/h. The average relative error between the simulation test and bench test was 2.33% when the forward speed of the planter was from 4 km/h to 16 km/h. The result of the bench test at the forward speed of the planter of 4-16 km/h showed that the designed seed metering device could meet high-speed and precision planting requirements.

Compared with the seed metering device designed by Shen et al. (2021), the high-speed and precision metering device with GF and CS could adapt to a broader range of speeds (4-16 km/h VS 8-15 km/h). All quality indices were higher than the corresponding results of Shen et al. (2021) when the forward speed of the planter was from 8 km/h to 15 km/h. All miss indices were lower than their corresponding results when the forward speed of the planter was 8 km/h to 15 km/h. It was proved that GF and CS structures effectively improved the quality index and reduced the miss index.

Conclusions

High-speed and precision metering device with GF and CS was designed for realizing high-speed and precision planting. Specific conclusions were as follows:

(1) A high-speed and precision metering device with GF and CS was designed to aim at the problems of slowly feeding seeds and over-clearing the mechanical seed metering device. The structure of GF was employed to feed seeds rapidly. The structure of CS reduced the phenomenon of over-clearing during the clearing stage.

(2) Through analyses and modeling, the optimal working parameters of high-speed and precision metering device with GF and CS were the angle of guiding-slope α = 18.06°, the angle of control-seed θ = 136.67°, and the mutation height ΔH = 2.77 mm. When the forward speed of the planter

was 8 km/h, simulation results showed that the quality index and the miss index of high-speed and precision metering device with GF and CS were 99.56% and 0.41%, respectively.

(3) For the designed high-speed and precision metering device with GF and CS, all quality indices of the bench tests were above 95.00% when the forward speed of the planter was from 4 km/h to 16 km/h. All miss indices of the bench test were lower than 3.00% at the same time. Bench test results were consistent with simulation results

Consequently, high-speed and precision metering device with GF and CS designed in this study was able to work for high-speed and precision planting conditions.

References

Ahmadi E., Ghassemzadeh H. R., Moghaddam M., Kim K. U. 2008. Development of a precision seed drill for oilseed rape. Turk. J. Agric. For. 32:451-458.

Cay A., Kocabiyik H., May S. 2018. Development of an electro-mechanic control system for seed-metering unit of single seed corn planters part II: Field performance. Comput. Electron. Agric. 145:11-17.

Chen Y., Jia H., Wang J., Wang Q., Hu B. 2017. Design and experiment of scoop metering device for soybean high-speed and precision seeder. Trans. Chin. Soc. Agric. Mach. 48:95-104.

Correia T. P. D. S., Sousa S. F. G. D., Silva P. R., Dias P. P., Gomes, A. R. A. 2016. Sowing performance by a metering mechanism of continuous flow in different slope conditions. Engenharia Agrícola. 36:839-845.

Du R., Gong B., Liu N., Wang C., Yang Z., Ma M. 2013. A Design and experiment on intelligent fuzzy monitoring system for corn planters. Intl. J. Agric. Biol. Eng. 6:11-18.

Du X., Liu C., Jiang M., Zhang F., Yuan H., Yang H. 2019. Design and experiment of self-disturbance inner-filling cell wheel maize precision seed-metering device. Trans. CSAE. 35:23-34. [In Chinese].

Gao X., Zhou Z., Xu Y., Yu Y, Su Y., Cui T. 2020. Numerical simulation of particle motion characteristics in quantitative seed feeding system. Powder Technol. 367:643-658.

He S., Zang Y., Huang Z., Tao W., Xing H., Qin W., Jiang Y., Wang Z. 2022. Design of and experiment on a cleaning mechanism of the pneumatic single seed metering device for coated hybrid rice. Agric. 12:1239.

Hu M., Xia J., Zheng K., Du J., Liu Z., Zhou M. 2021. Design and experiment of inside-filling

pneumatic high speed precision seed-metering device for cotton. Trans. Chin. Soc. Agric. Mach. 52:73-85. [In Chinese].

Hu M., Xia J., Zhou M., Liu Z., Xie D. 2022. Design and experiment of seed-cleaning mechanism for inside-filling pneumatic cotton precision seed-metering device. Agric. 12:1217.

Jia H., Chen Y, Zhao J., Guo M, Huang D, Zhuang J. 2018. Design and key parameter optimization of an agitated soybean seed metering device with horizontal seed filling. Intl. J. Agric. Biol. Eng. 11:76-87.

Khatchatourian O. A., Binelo M. O., De Lima R. F. 2014. Simulation of soya bean flow in mixed-flow dryers using DEM. Biosyst. Eng. 123:68-76.

Koller A., Wan Y., Miller E., Weckler P., Taylor R. 2014. Test method for precision seed singulation systems. Trans. ASABE. 57:1283-1290.

Kostic M., Rakic D., Radomirovic D., Savin L., Dedovic N., Crnojevic V., Ljubicic N. 2018. Corn seeding process fault cause analysis based on a theoretical and experimental approach. Comput. Electron. Agric. 151:207-218.

Li Y., Wei Y., Yang L., Zhang D., Cui T., Zhang K. 2020. Design and experiment of mung bean precision seed-metering device with disturbance for promoting seed filling. Trans. Chin. Soc. Agric. Mach. 51:43-53. [In Chinese].

Liu H., Guo L., Fu L., Tang S. 2015. Study on multi-size seed-metering device for vertical plate soybean precision planter. Intl. J. Agric. Biol. Eng. 8:1-8.

Ryu I. H., Kim K. U. 1998. Design of roller type metering device for precision planting. Trans. ASAE. 41:923-930.

Sharaby N., Doroshenko A., Butovchenko A. 2022. Modelling and verification of sesame seed particles using the discrete element method. J. Agric. Eng. 53:1286.

Shen H., Zhang J., Chen X., Dong J., Huang Y., Shi J. 2021. Development of a guiding-groove precision metering device for high-speed planting of soybean. Trans. ASABE. 64:1113-1122.

Wang J., Qi X., Xu C., Wang Z., Jiang Y., Tang H. 2021. Design evaluation and performance analysis of the inside-filling air-assisted high-speed precision maize seed-metering device. Sustainability. 13:5483.

Wang J., Tang H., Guan R., Li X., Bai H., Tian L. 2017. Optimization design and experiment on clamping static and dynamic finger-spoon maize precision seed metering device. Trans. Chin. Soc.

Agric. Mach. 48:48-57. [In Chinese].

Wang W., Wu K., Zhang Y., Wang M., Zhang C., Chen L. 2022. The development of an electric-driven control system for a high-speed precision planter based on the double closed-loop fuzzy PID algorithm. Agronomy-Basel. 12:945.

Wang W., Zhang S., Li J., Zhang P., Chen Y. 2022. Effects of the win-row planter with subsoiling on soybean growth and yield in northern China. J. Agric. Eng. 53: 1359.

Xing H., Zang Y., Wang M., Luo W., Zhang H., Fang Y. 2020. Design and experimental analysis of a stirring device for a pneumatic precision rice seed metering device. Trans. ASABE. 63:799-808.

Xiong D., Wu M., Xie W., Liu R., Luo H. 2021. Design and experimental study of the general mechanical pneumatic combined seed metering device. Appl. Sci. 11:7223.

Xue P., Hao Y., Jiao W., Ren J., Huang Y. 2020. Design and test of a double-curved guiding groove for a high-speed precision seed-metering device. Trans. ASABE. 63:1349-1360.

Xue P., Xia X., Gao P., Ren D., Hao Y., Zheng Z., Zhang J., Zhu R., Hu B., Huang Y. 2019. Double-setting seed-metering device for precision planting of soybean at high speeds. Trans. ASABE. 62:187-196.

Yazgi A., Degirmencioglu A. 2007. Optimisation of the seed spacing uniformity performance of a vacuum-type precision seeder using response surface methodology. Biosyst. Eng. 97:347-356.

Zhao J., Zhen C., Zhang J., Hang D., Nian Y., Sun N. 2020. Parameter optimization and experiment of differential filling groove single grain seed metering device for wheat. Trans. Chin. Soc. Agric. Mach. 51:65-74. [In Chinese].

Zhao X., Ran W., Hao J., Bai W., Yang X. 2022. Design and experiment of the double-seed hole seeding precision seed metering device for peanuts. Intl. J. Agric. Biol. Eng. 15:107-114.

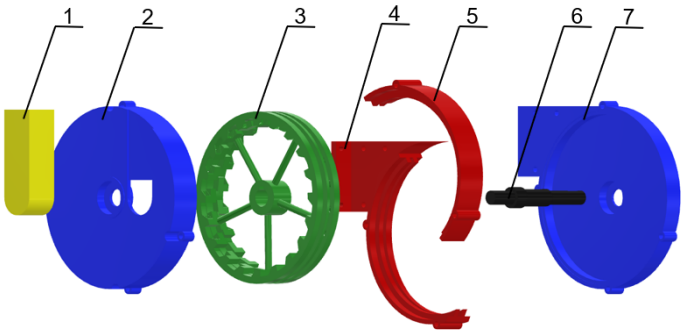

(a)

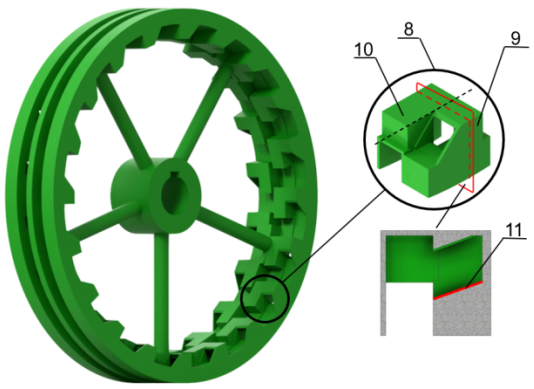

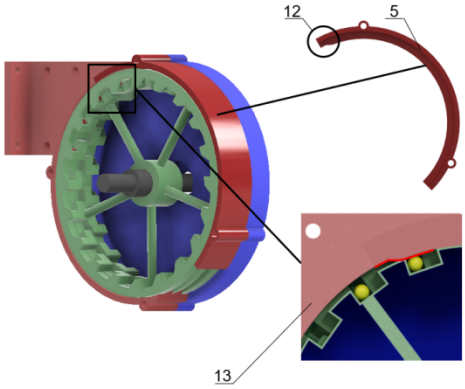

(b) (c)

Figure 1. Structure of high-speed and precision metering device. (a) components of high-speed and precision metering device, (b) seed cell of the seed-taking wheel, and (c) control-seed of high-speed and precision metering device, (1 = seed feeding tube, 2 = front shell, 3 = seed-taking wheel, 4 = fixed limiting ring, 5 = adjusting limiting ring, 6 = transmission shaft, 7 = rear shell, 8 = seed cell, 9 = seed-feeding chamber, 10 = seed-releasing chamber, 11 = guiding-slope, 12 = mutation structure, 13 = control-seed).

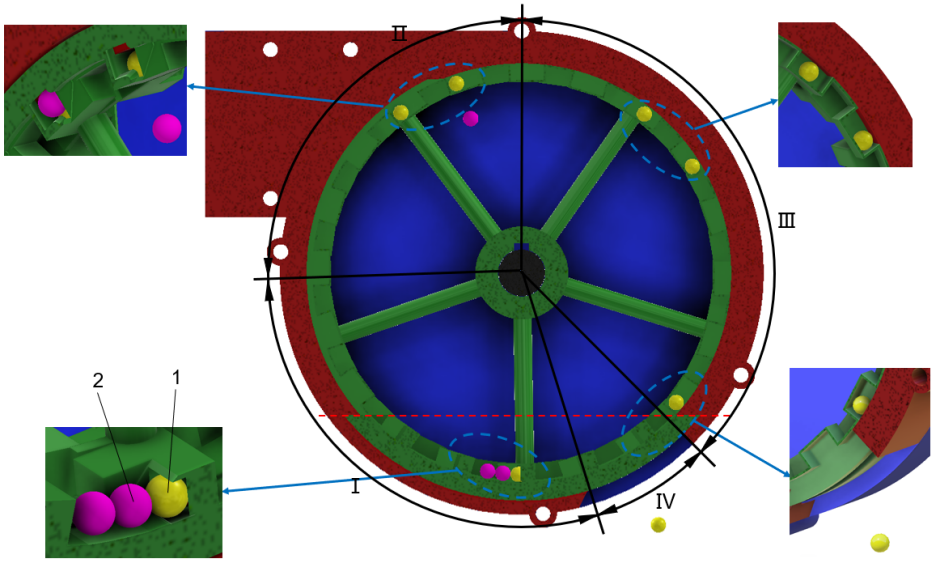

Figure 2. Diagram of working principle of the high-speed and precision metering device (I = feeding stage, II = clearing stage, III = protecting stage, IV = releasing stage). (1 = the seed to be released, 2= the seed to be cleared).

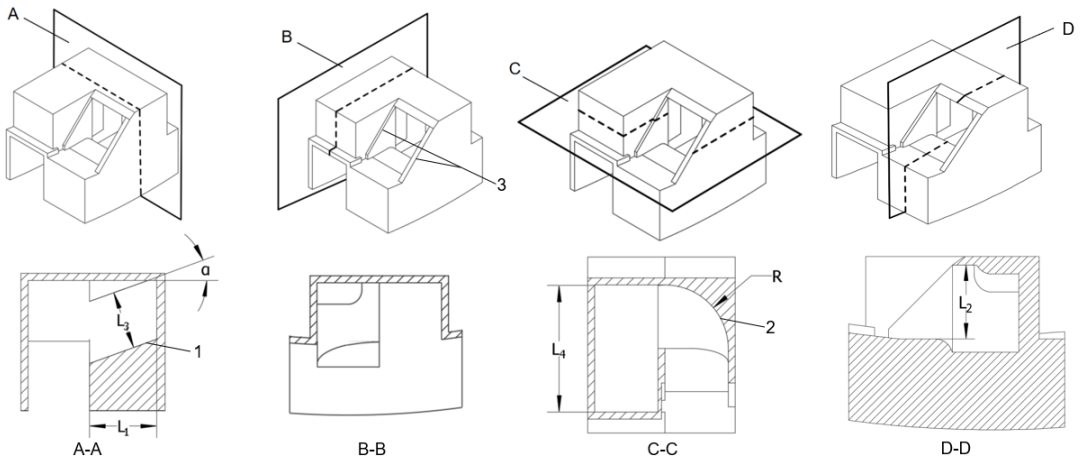

Figure 3. The sectional view of the seed cell (1 = guiding-slope, 2 = arc surface, 3 = inclined side plate).

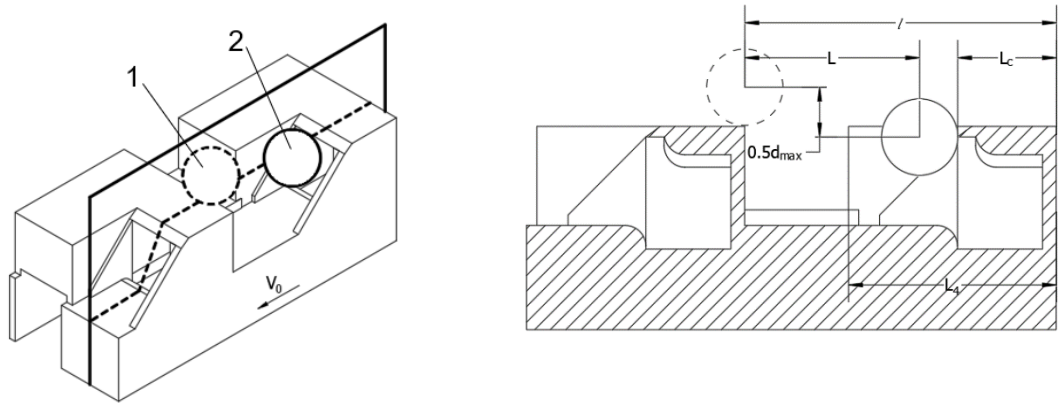

(a) (b)

Figure 4. Distribution of seed cells (a) Three-dimensional diagram of seed cell distribution distance and (b) Profile of seed cell distribution distance. (1 = former position of soybean seed before it fell due to gravity and speed of the seed-taking wheel (v_0), 2 = current position of this soybean seed).

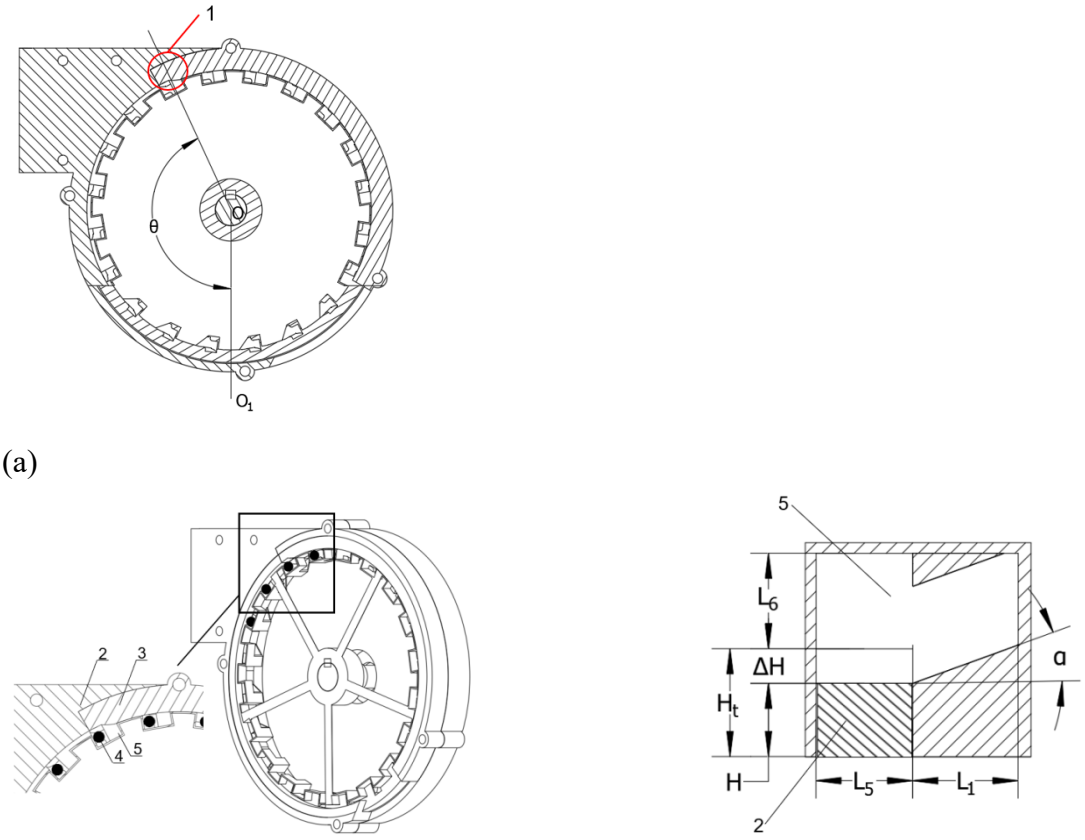

Figure 5. The structure of control-seed (a) angle of seed control, (b) schematic diagram of control-seed, (c) sectional view of the control-seed structure. (1 = fixed limiting ring, 2 = adjusting limiting ring, 3 = seed cell, 4 = seeds, 5 = mutation structure).

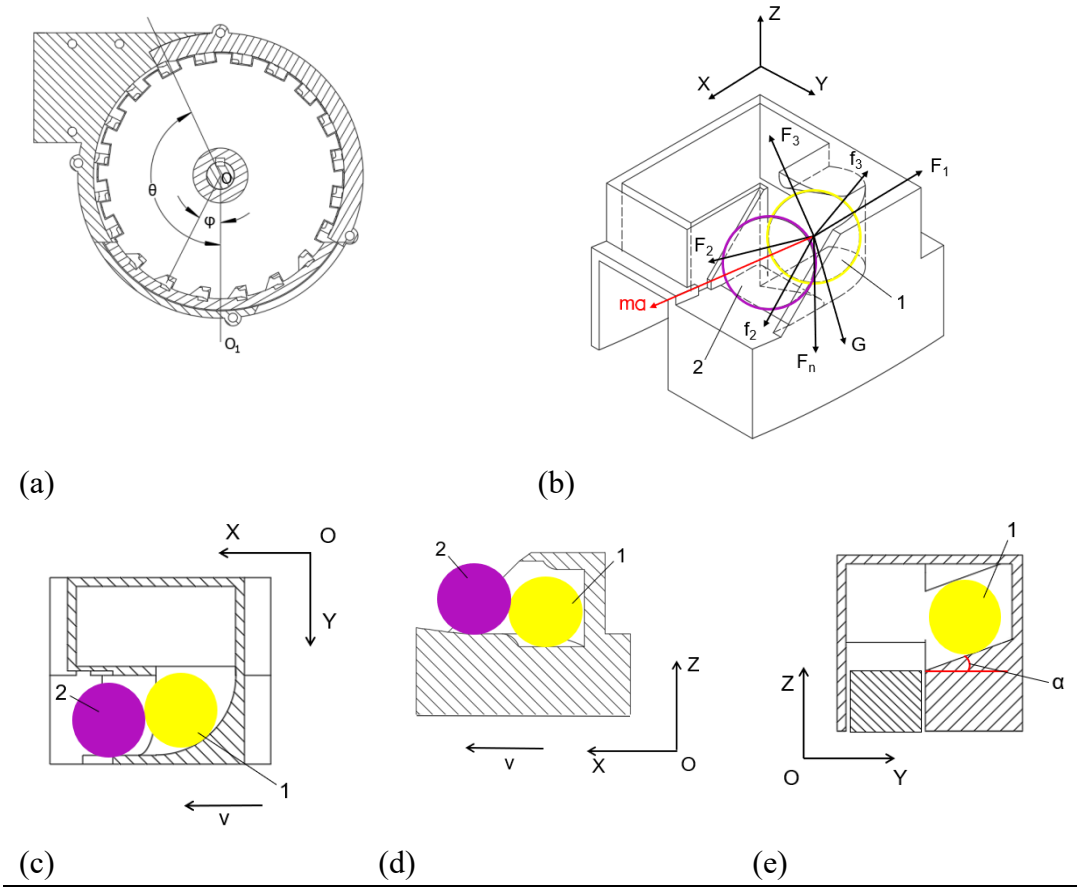

Figure 6. (a) Position angle diagram of the seed cell, (b) analysis diagram of seeding stage in XYZ plan, (c) analysis diagram of seeding stage in XOY plan, (d) analysis diagram of feeding stage in XOZ plan, (e) analysis diagram of feeding stage in YOZ plan. (1 = the seed to be released, 2= the seed to be cleared).

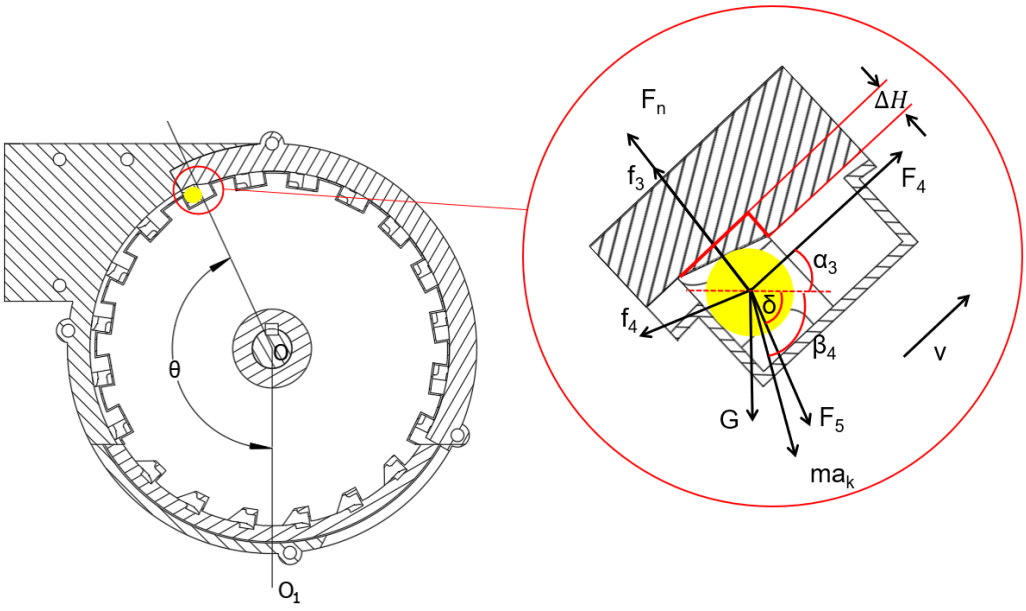

Figure 7. Force analysis during control-seed process.

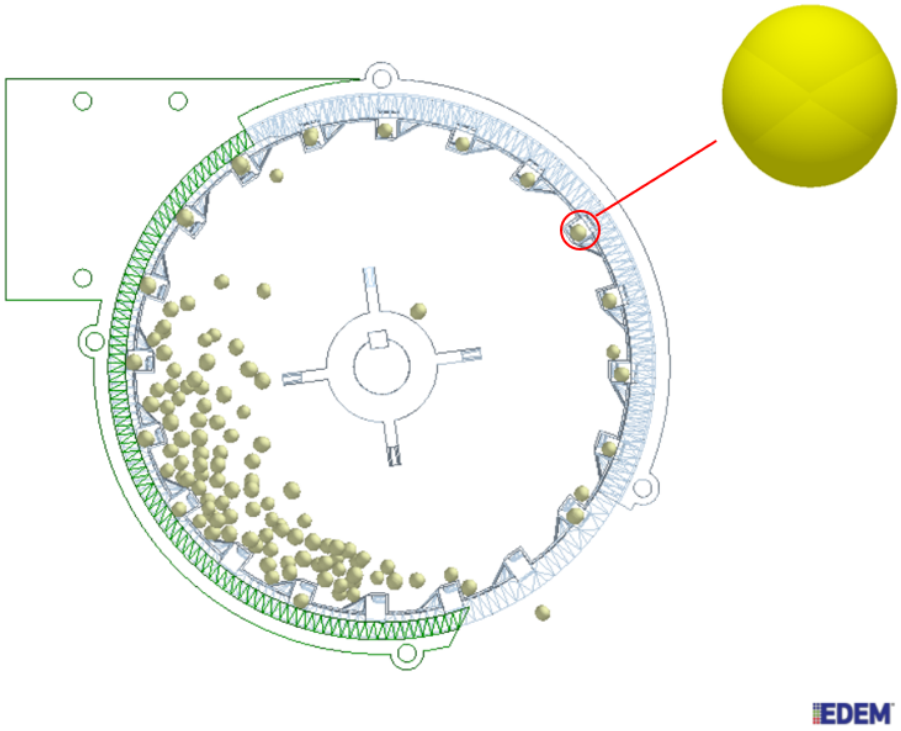

Figure 8. Digital modeling of the high-speed and precision metering device with GF and CS in EDEM.

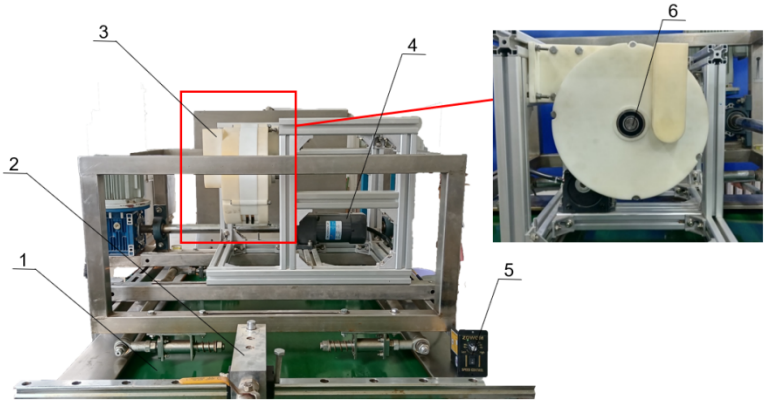

(a)

(b) (c)

Figure 9. Bench test: (a) high-speed and precision metering device, (b) seed metering effect, and (c) distance between soybean seeds measured with a ruler (1 = oil belt, 2 = oil pump, 3 = the model of high-speed and precision metering device, 4 = motor, 5 = controller, 6 = transmission shaft).

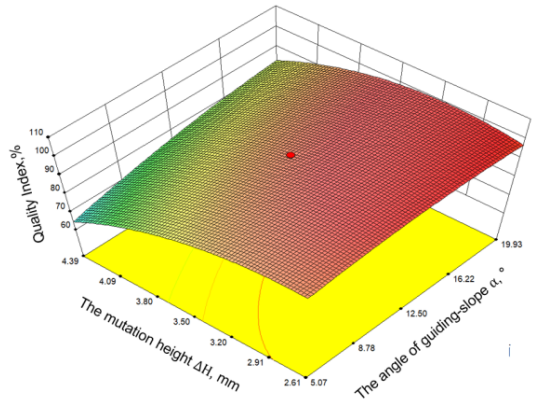

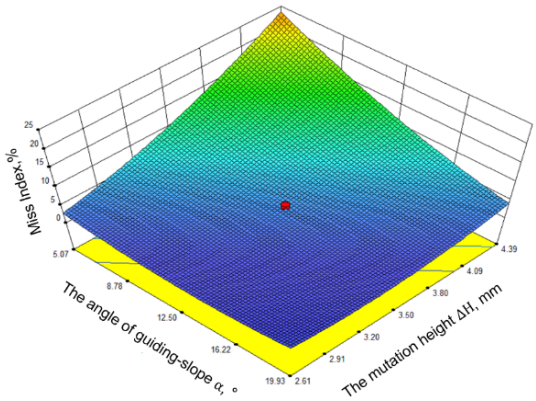

(a) (b)

Figure 10. Response surfaces of quality index (I_q) and miss index (I_m) for different design parameters.

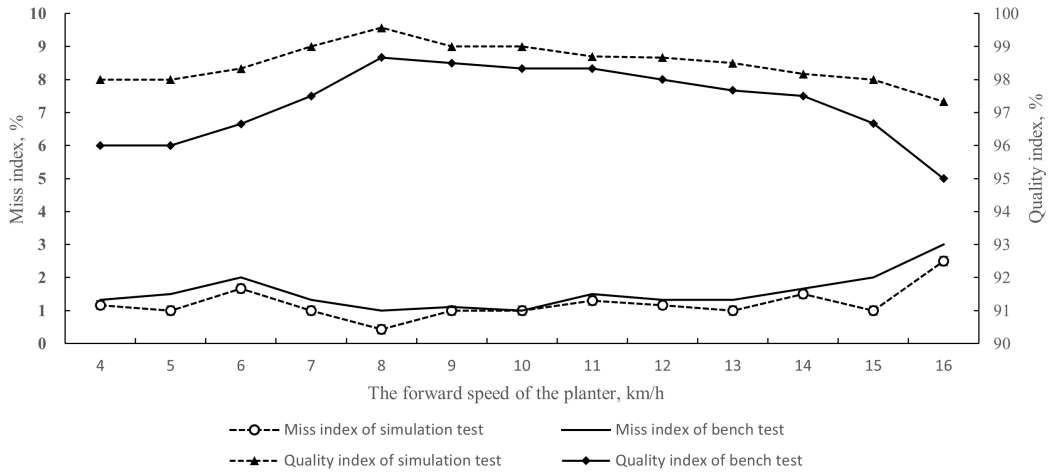

Figure 11. Verification results of the bench test.

Table 1. Model input parameters used in simulations.

Category	Parameter	Value
Seed	Poisson's ratio	0.25
	Shear modulus (Pa)	6.12×105
	Density (kg m-3)	1267
Machine	Poisson's ratio	0.28
	Shear modulus (Pa)	8.2×1010
	Density (kg m-3)	7890
Seed-seed interaction	Coefficient of restitution	0.55
	Dynamic friction coefficient	0.45
	Rolling friction coefficient	0.06
Seed-machine interaction	Coefficient of restitution	0.52
	Dynamic friction coefficient	0.50
	Rolling friction coefficient	0. 1

Table 2. Triaxial size parameters of soybean seeds.

Characteristic	Length (mm)	Width (mm)	Thickness (mm)	Volume equivalent diameter (mm)
Mean	7.42	6.86	7.32	7.20
SD	0.43	0.30	0.26	0.33
Size range	6.56 – 8.93	5.96 – 7.59	6.59 - 8.13	6.37 – 8.22 (d_{min} -

				d_{max})

Table 3. Coded levels for independent variables.

Variable	Code	Coded Levels				
		-1.681	-1	0	+1	+1.681
α(°)	A	0	5.07	12.50	19.93	25.00
θ(°)	B	90.00	108.24	135.00	161.76	180.00
ΔH(mm)	C	2.00	2.61	3.50	4.39	5.00

Table 4. Simulation test scheme and results.

Combination	Independent Variables			Performance Indices	
	A(α, °)	B(θ, °)	C(ΔH, mm)	(I_q, %)	(I_m, %)
1	5.07	108.24	2.61	91.00	5.00
2	19.93	108.24	2.61	96.33	2.00
3	5.07	161.76	2.61	95.67	2.00
4	19.93	161.76	2.61	95.00	1.67
5	5.07	108.24	4.39	60.00	27.67
6	19.93	108.24	4.39	81.33	6.33
7	5.07	161.76	4.39	67.67	21.67
8	19.93	161.76	4.39	85.00	3.67
9	0.00	135.00	3.50	81.00	17.67
10	25.00	135.00	3.50	98.67	0.67
11	12.50	90.00	3.50	91.00	8.00
12	12.50	180.00	3.50	97.67	2.33
13	12.50	135.00	2.00	92.00	1.00
14	12.50	135.00	5.00	53.33	19.67
15	12.50	135.00	3.50	96.00	4.00
16	12.50	135.00	3.50	95.33	4.67
17	12.50	135.00	3.50	96.67	3.33
18	12.50	135.00	3.50	96.67	3.33
19	12.50	135.00	3.50	96.67	3.22
20	12.50	135.00	3.50	96.67	3.33

Table 5. Significance of factors for performance indices.

Source	Performance Indices	
	I_q (%)	I_m (%)
	Prob > F	Prob > F
Model	<0.0001**	<0.0001**
A	<0.0001**	<0.0001**
B	<0.0001**	<0.0001**
C	<0.0001**	<0.0001**
AB	0.0033*	0.0038*
AC	<0.0001**	<0.0001**
BC	0.0118	0.0078*
A^2	<0.0001**	<0.0001**
B^2	0.0038*	0.0028*
C^2	<0.0001**	<0.0001**
Lack of fit	0.0651	0.5216
Note: * Indicates significance at P<0.01, ** Indicates significance at p<0.001.		